The American Journal of Pathology, Vol. 169, No. 5, November 2006

DOI: 10.2353/ajpath.2006.051222

Tumorigenesis and Neoplastic Progression

Preferential Attachment of Peritoneal Tumor Metastases to Omental Immune Aggregates and Possible Role of a Unique Vascular Microenvironment in Metastatic Survival and Growth

Scott A. Gerber,* Viktoriya Y. Rybalko,* Chad E. Bigelow,† Amit A. Lugade,* Thomas H. Foster,† John G. Frelinger,* and Edith M. Lord*

From the Departments of Microbiology and Immunology and Imaging Sciences,† University of Rochester Medical Center, Rochester, New York*

Controlling metastases remains a critical problem in cancer biology. Within the peritoneal cavity, omental tissue is a common site for metastatic disease arising from intraperitoneal tumors; however, it is unknown why this tissue is so favorable for metastatic tumor growth. Using five different tumor cell lines in three different strains of mice, we found that the omentum was a major site of metastases growth for intraperitoneal tumors. Furthermore, initial attachment and subsequent growth were limited to specific sites within the omentum, consisting of organized aggregates of immune cells. These immune aggregates contained a complex network of capillaries exhibiting a high vascular density, which appear to contribute to the survival of metastatic cells. We found that the vasculature within these aggregates contained CD105$^+$ vessels and vascular sprouts, both indicators of active angiogenesis. A subset of mesothelial cells situated atop the immune aggregates was found to be hypoxic, and a similar proportion was observed to secrete vascular endothelial growth factor-A. These data provide a physiological mechanism by which metastatic tumor cells preferentially grow at sites rich in proangiogenic vessels, apparently stimulated by angiogenic factors produced by mesothelial cells. These sites provide metastatic cells with a microenvironment highly conducive to survival and subsequent growth. ***(Am J Pathol 2006, 169:1739–1752; DOI: 10.2353/ajpath.2006.051222)***

Malignant cells often metastasize into the peritoneal cavity from intra-abdominal primary tumors including ovarian, colon, and stomach.[1–3] For these intra-abdominal tumors, direct intraperitoneal seeding is a common avenue of metastatic dissemination, although lymphatic and hematogenous spread can also occur. This direct seeding can arise when tumor cells are dislodged from the primary neoplasm, either naturally or during the process of surgical tumor resection, and the natural flow of peritoneal fluid then transports these malignant cells throughout the abdomen.[2,4] This metastatic stage of disease is frequently characterized by aggressive tumor growth resulting in a poor prognosis.

A peritoneal tissue of particular interest is the omentum because it is a common site of metastatic tumor foci in patients.[2,4–8] The gross anatomy of the omentum varies somewhat among species, but it typically drapes off of the stomach and consists of membranous layers of adipose tissue with aggregates of leukocytes interspersed among fat cells.[9–11] Ranvier[12] in 1874 was the first to describe these immune aggregates, which he termed milky spots, on the omentum of rabbits. Since then, omental immune aggregates have been observed in many mammals, including humans.[10] These aggregates appear to respond to bacterial antigens or other forms of peritoneal stimuli by local lymphocyte proliferation, along with a rapid influx of effector cells from the blood stream or peritoneal cavity[13–15] and may be involved in host defense. Interestingly, surgical removal of the omentum often leads to impaired anti-bacterial responses within the peritoneal cavity.[9] These omental immune aggregates are also sites of macrophage maturation and of development of the self-renewing B-1 B cells, specialized

Supported by the National Institutes of Health (training grant AI07285 to S.A.G. and A.A.L. and grant CA28332).

Accepted for publication July 18, 2006.

Address reprint requests to Edith M. Lord, Ph.D., University of Rochester, 601 Elmwood Ave., Box 672, Rochester, NY 14620. E-mail: edith_lord@urmc.rochester.edu.

B cells that produce low-affinity IgM natural antibodies.[14,16–18] Surprisingly, the precise physiological function and cellular composition of the immune aggregates within the omentum are poorly understood. Despite this apparent immune function, tumor cells can bind to the aggregates, suggesting that these sites may play an important role in peritoneal metastatic disease.[5,6,19,20]

A primary tumor may shed a large number of metastatic tumor cells each day, yet only a few of these cells will actually develop into metastases.[21] Metastatic development is dependent on the acquisition of traits that promote survival by the tumor cells themselves as well as properties of the target tissue.[22] One particularly important component in this multistep process is the vascular system. For tumors in most anatomical locations, there is strong evidence that the rate of metastases is greater from highly vascularized primary tumors because there is greater opportunity for metastatic cells to escape into the circulation.[23] However, for intraperitoneal tumors in which metastases occur primarily by direct seeding rather than via the circulation, the vasculature may have an alternate role. In this case high levels of vascularization within the host tissue microenvironment may be the more important criteria contributing to metastatic survival.[17,21,24] Metastatic tumor cells have been found to migrate toward the closest microvessel and there start dividing.[25] These findings suggest that metastatic cells that seed in well-vascularized areas have a survival advantage that can result in more aggressive tumor growth. This hypothesis is further supported by clinical observation that aggressive metastases are most commonly found in well-vascularized tissues such as the lung, liver, and brain.[26]

Here we find that a variety of tumor cell types injected into the peritoneal cavity preferentially attach to immune aggregates on the omentum and mesentery. In addition to this rapid and selective attachment, these sites exhibit a unique vascular microenvironment that appears to promote metastatic survival and subsequent tumor growth. A more comprehensive understanding of the factors involved in making these sites favorable to tumor growth could lead to better therapies for malignant cancer.

Materials and Methods

Mice and Removal/Processing of Omenta

C57BL/6, BALB/cByJ, and C3H/HeJ mice (6 to 10 weeks of age) purchased from The Jackson Laboratory (Bar Harbor, ME) were treated using guidelines approved by the University Committee on Animal Resources. Mice were sacrificed, and the majority of the greater omentum from the hilum of the spleen, along the curvature of the stomach, to the edge of the pancreas was surgically removed. Tissue was placed in cold phosphate-buffered saline (PBS) (Sigma, St. Louis, MO) and examined by fluorescence microscopy or dissociated to obtain a single cell suspension. In brief, naïve omenta were minced in 2 ml of 0.2% collagenase (Sigma) with rotation at 37°C for 45 minutes. Samples were filtered using a 40-μm nylon cell strainer (Becton-Dickinson, Mountain View, CA), and undigested pieces were further dissociated by rubbing between two frosted slides.

Cell Lines

All cells were maintained in MAT/P media (US patent no. 4.816.401) supplemented with 100 U/ml^{-1} penicillin, 100 mg/ml^{-1} streptomycin, and either 2% (tumor lines) or 5% (cells from omental and lymphoid tissues) fetal calf serum. Tumor cell lines used included B16 (syngeneic with C57BL/6 H-2^b, melanoma), Line1 (syngeneic with BALB/c mice H-2^d, lung carcinoma), EMT6 (syngeneic with BALB/c mice, mammary carcinoma), K1735.1 (syngeneic with C3H/HeJ mice H-2^k, melanoma), and ID8 (syngeneic with C57BL/6, ovarian carcinoma). The pEGFP-Neo plasmid was transfected into each cell line using Lipofectin (BRL, Gaithersburg, MD), according to the manufacturer's directions. Cells expressing the highest level of green fluorescent protein (GFP), as determined by flow cytometry, were selected by subcloning.

Whole Mount Analysis and Fluorescence Microscopy

Primary and secondary antibodies used for whole mount immunocytochemistry are listed in Table 1. Whole mount histology was performed as previously described.[27,28] In brief, the greater omentum was blocked using Fc Block (BD Biosciences, San Diego, CA) at 10 μg/ml in 200 μl of PBA (PBS with 1% bovine serum albumin and 0.1% sodium azide) with shaking at 4°C for 10 minutes. Additional blocking procedures were added when mouse secondary antibodies were used to detect anti-CD105 or anti-LYVE-1, which included preblocking the tissue in Fc block at 10 μg/ml in 200 μl of PBA + 5% normal mouse serum (Jackson ImmunoResearch, West Grove, PA). After blocking, primary antibody was added directly to the tube for 2 hours, after which samples were washed and mounted on a slide. When required, a secondary antibody was added after the first wash step for an additional 2 hours and washed similarly. The samples were viewed by fluorescence microscopy, and digital images were acquired using fluorescence filter cubes as described elsewhere.[28] Digital images were pseudo-colored, overlaid, and analyzed using Image Pro Plus software Version 5.0 (Media Cybernetics, Baltimore, MD). To examine tumor growth kinetics, a defined number of B16 or B16/GFP tumor cells was washed in Hanks' balanced salt solution and injected intraperitoneally into syngeneic mice. At 10 hours or 2, 4, 6, or 8 days after injection, omenta were removed, stained with antibodies, and visualized for amount and location of tumor growth using whole mount histology.

Confocal Analysis of the Omentum

Naïve omenta were stained simultaneously with anti-CD45-fluorescein isothiocyanate and anti-VCAM-PE

Table 1. Antibodies Used

Primary antibody name	Clone	Concentration (μg/ml)	Source
Anti-CD4-PE/PerCP	RM4-5	4	BD Biosciences
Anti-CD5-PE	53-7.3	4	BD Biosciences
Anti-CD8-FITC/PerCP	53-6.7	4	BD Biosciences
Anti-CD11b-FITC/PerCP	M1/70	1	BD Biosciences
Anti-CD11c-PE	HL3	2.5	BD Biosciences
Anti-CD19-APC	1D3	3	BD Biosciences
Anti-CD31-FITC/PE/APC	MEC 13.3	10	BD Biosciences
Anti-CD44-APC	IM7	4	BD Biosciences
Anti-CD45-FITC/PE/APC	30-F11	1.25	BD Biosciences
Anti-CD105	MJ7/18	5	BD Biosciences
Anti-CD106 (VCAM-1)-FITC/biotin	429	10	BD/eBioscience
Anti-collagen type IV	Goat poly	4	Southern Biotech
Anti-NK1.1-PE	PK136	4	BD Biosciences
Anti-F4/80-APC	BM8	2	EBioscience
Anti-GR-1-PE	RB6-8C5	4	BD Biosciences
Fc block	2.462	10	BD Biosciences
Anti-LYVE-1	Rabbit poly	2	Dr. David Jackson
Anti-PNAd	MECA-79	7.5	BD Biosciences
Isotype rat IgG2b	Rat		BD Biosciences
Isotype rat IgG2a	Rat		BD Biosciences
Isotype hamster IgG	Hamster		BD Biosciences

Secondary reagent	Used to detect	Dilution	Source
Streptavidin-PerCP	Biotin-conjugated antibodies	1:200	BD Biosciences
Goat anti-rat-IgM-Cy3	Anti-PNAd	1:500	Jackson ImmunoResearch Labs
Mouse anti-rabbit-IgG-Cy3	Anti-LYVE-1	1:500	Jackson ImmunoResearch Labs
Mouse anti-rat-IgG-Cy3	Anti-CD105	1:600	Jackson ImmunoResearch Labs
Donkey anti-goat-Cy3	Anti-collagen IV	1:500	Jackson ImmunoResearch Labs

and prepared as whole mounts. Confocal fluorescence analysis of individual immune aggregates was performed using a custom confocal microscope.[29] To determine the relative orientation of the $CD45^+$ cells to the $VCAM^+$ cells, 2-μm axial sections starting above the aggregate and descending into the underlying layer of adipose tissue were obtained from each immune aggregate. Images consisting of 800 $\times$ 800-μm fields of view with pixel arrays of 600 $\times$ 600 from the two fluorescence channels were digitized at 16 bits, pseudo-colored, and overlaid.

Image Analysis: Vascular Density and Enumeration of Vascular Sprouts

For the vessel density studies, three individual omenta were stained with anti-CD31 antibody to label blood vessels and anti-CD45 antibody to allow localization of the immune aggregates, and 15 corresponding 10$\times$ digital images were obtained from each omentum. Percent vessel area within immune aggregates was determined by segmenting the $CD31^+$ images using a predefined color range, selected to allow detection of all vessels regardless of CD31 intensity, to form a binary image of blood vessels. Regions of interest around the vessels within or immediately surrounding the aggregate and outside the aggregate were drawn and computed to determine the percent vessel area. The values for each region were averaged and SEM calculated.

Vascular sprouts, defined as branched vessel-like structures that did not coalesce with another vessel at one end, were counted manually using collagen IV as the marker. Using the digital images, the area of each aggregate was computed by Image Pro Plus software. For each aggregate, the number of sprouts was divided by the area of that particular aggregate and then multiplied by the average area of all aggregates (calculated to be 188 mm^2). This allowed standardization of the results to the number of sprouts per unit area. The arithmetic mean and SEM were subsequently calculated.

Vascular Endothelial Growth Factor (VEGF)-A Quantification Using Enzyme-Linked Immunosorbent Assay (ELISA)

Single cell suspensions of omentum, peritoneal lavage, mesenteric lymph nodes, and spleen were plated at 10^6 cells in 300 μl of media in 24-well plates (Corning, Corning, NY) and incubated in normoxic (21% oxygen) conditions at 37°C. A duplicate plate was placed in a hypoxic chamber that was subjected to six 90% gas exchanges

with nitrogen/5% carbon dioxide mix and then placed at 37°C. Supernatants were collected after 16 hours because this was sufficient time for accumulation of secreted VEGF-A, whose levels were then determined by ELISA (PeproTech, Rocky Hill, NJ). Mesothelial cells ($VCAM^+$, $CD45^-$) and $CD45^+$ cells were isolated from omental single-cell suspensions by simultaneously sorting on an EPICS Elite ESP Sorter (Beckman Coulter, Fullerton, CA). The cell populations were cultured as above, and the supernatant was assayed for VEGF-A.

Intracellular Staining for VEGF-A and EF5

Intracellular staining for VEGF-A was performed on single cell suspensions from both the peritoneal lavage and omental cells cultured for 16 hours with and without brefeldin A [Golgi plug (GP); Becton-Dickinson] under either normoxic or hypoxic conditions, and then the cells were removed and stained for surface markers as described above. Antibodies used for flow cytometry are listed in Table 1. After the cells were fixed and permeabilized using the CytoPerm/CytoWash kit (BD Biosciences), cells were blocked in 7% normal rat serum (Sigma), and VEGF-A was detected with a biotinylated antibody and streptavidin-PerCP. Streptavidin-PerCP alone was used as a negative control. The amount of intracellular VEGF-A was determined as the mean fluorescent intensity of VEGF-A staining/mean fluorescent intensity of the secondary alone for each immune subset from each culture condition (normoxic, normoxic + GP, hypoxic + GP). The values obtained in the presence of GP were then divided by the negative control (normoxic without GP) and reported as the fold increase. This calculation was performed on each immune subset from three separate experiments and the arithmetic mean and SEM calculated.

EF5, the kind gift of Dr. Cameron Koch, University of Pennsylvania, Philadelphia, PA, was used to detect hypoxic cells[30] from omental single cell suspensions. Mice were injected intraperitoneally with 250 μl of a 10 mmol/L solution of EF5 in sterile PBS or sterile PBS alone (no drug control). Three hours later, omenta were removed, and single cell suspensions prepared and stained with ELK3-51-Cy3, a monoclonal antibody specific for EF5. Specific gated populations from the EF5-injected and the no drug mice were compared for ELK3-51-Cy3 intensity. Hypoxic fractions were defined as the percent positive over the no drug control.

Statistical Analysis

Data were analyzed using InStat (GraphPad, San Diego, CA) software. The Wilcoxon signed rank sum test or analysis of variance followed by the Bonferroni multiple comparison test was performed to test for significance. Using 95% confidence limits, P values of <0.05 were considered to indicate statistically significant differences.

Results

Tumor Cells Exhibit Selective Attachment and Growth on Specific Sites within Peritoneal Tissues

To examine which tissues are key sites for peritoneal metastatic growth, naïve C57BL/6 mice were injected intraperitoneally with B16 melanoma cells. This cell line contains melanin and grows as distinct dark foci on tissues, which are easily visible by eye. Figure 1A is representative of a mouse abdomen 6 days after injection, illustrating the presence of abundant tumor on the omentum (arrow), along with multiple smaller foci on peritoneal adipose tissue and the mesentery (inset). Tumor growth was not visible on any other major organs or tissues at this time point. This selective growth on the omentum and mesentery was not limited to B16 because four additional tumor cell lines, expressing GFP to facilitate detection at the microscopic level, exhibited growth predominately on the omentum along with smaller foci on the mesentery (data not shown). These cell lines included a melanoma of C3H origin, a lung and a breast carcinoma, both syngeneic with BALB/c, and a C57BL/6-derived ovarian tumor, indicting that this selective growth is not a characteristic of a single tumor cell type. In a more extensive experiment, these same five cell lines were injected intraperitoneally, and 3 days later, multiple organs were examined for the presence of metastatic cells. As expected, abundant foci were found on the omentum, whereas few metastatic foci were found on the diaphragm and pancreas and none in the liver, lungs, or kidney (data not shown). In addition, we also injected the GFP-expressing tumor cells intravenously and examined the omentum 1 and 3 days later. In marked contrast to the intraperitoneal injection, no GFP-positive cells were found on the immune aggregates 1 day after the intravenous injection of the cells and at 3 days only a few cells were visible (data not shown). These results suggest that the migration and attachment of the tumor cells occurs via direct migration from the peritoneal cavity rather than transport via the vascular system.

To characterize more fully this selective attachment and growth of tumor cells, we used multicolor whole mount histology[27,28] to examine the characteristics of the omentum and tumor attachment. Ten hours after injection of B16 tumor cells, the omentum was removed and stained using multiple antibodies described in Table 1. Figure 1B is a montage image of the entire omentum (outlined in white) depicting an overview of the immune cells and vascular networks associated with this tissue. Abundant $CD45^+$ immune aggregates (red) varying in size and shape can be observed in this image. Staining with CD31 (green) revealed large, centrally located blood vessels that branch into smaller arterioles/venules infiltrating each immune aggregate. Anti-LYVE-1 (yellow) was used to identify lymphatic vessels. A single central lymphatic was visible adjacent to the large blood vessel, but this vessel appeared to have blunt-ended processes that, unlike the blood vessels, did not extend into the

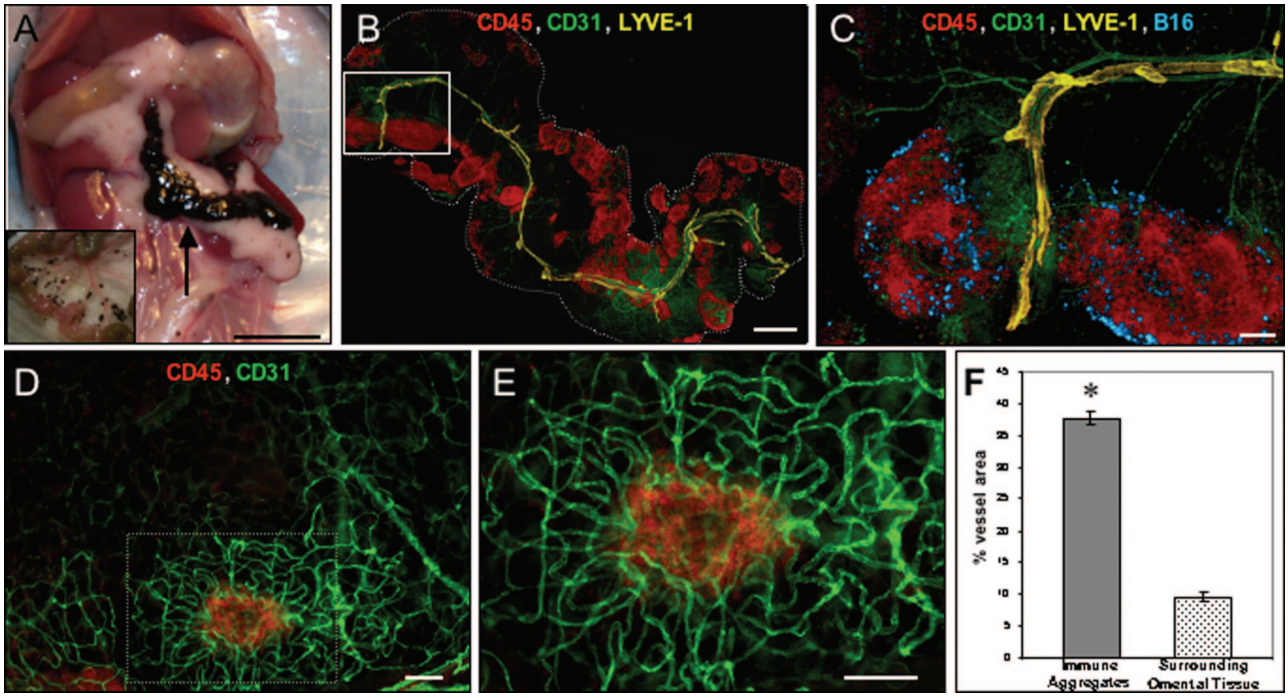

Figure 1. Tumor cells attach to vascular dense immune aggregates on the omentum. **A:** The growth of tumor within the peritoneal cavity of a mouse injected intraperitoneally 6 days earlier with 2×10^5 B16 tumor cells. The intestines were removed and are shown in the **inset**. **B:** An overview of the entire omentum from a mouse injected 10 hours earlier with 10^6 B16. The omentum was stained simultaneously with anti-CD45 to label immune cells (red), anti-CD31 to mark blood vessels (green), and anti-LYVE-1 (yellow) to identify lymphatic vessels. The tissue was prepared as a whole mount, viewed by fluorescence microscopy, and is shown as a montage overlay. **C:** Magnification of the white box, now including tumor cells (blue). **D** and **E:** An immune aggregate (anti-CD45-red) with a dense network of blood vessels (anti-CD31-green) (**D**) and at higher magnification (**E**). **F:** Image analysis of vascular density (percent vessel area) of the areas surrounding immune aggregates, such as the boxed area in **D** compared with surrounding areas. Images are representative of at least three independent experiments. *Significant at $P < 0.001$ as determined by the Wilcoxon signed rank test. Scale bars: 1 cm (**A**); 1 mm (**B**); 200 μm (**C**); 100 μm (**D**, **E**).

aggregates. An enlargement of two of these immune aggregates is shown in Figure 1C along with bound tumor cells (blue). Interestingly, the tumor cells are localized specifically to the $CD45^+$ immune aggregates and are not found on the surrounding areas of the omentum. Analysis of this binding at other time points revealed that the injected tumor cells were found attached in this pattern as soon as 1 hour after injection (data not shown), indicating that the initial attachment event is extremely rapid as well as selective. This pattern of attachment is not due solely to the injection of a bolus of tumor cells because injection of much smaller numbers of cells resulted in the same pattern of selective attachment to the immune aggregates (data not shown).

The vasculature associated with the immune aggregates, particularly the capillaries not readily visible at the magnification shown in Figure 1B, was analyzed in greater detail (Figure 1, D and E). These images illustrate morphologically distinct CD31-labeled blood vessels (green) that encircle each $CD45^+$ aggregate (red). Higher magnification (Figure 1E) reveals small capillary vessels that form a dense vascular network that commonly extends beyond the borders of the $CD45^+$ cluster. Segments of these vessels stained positively for the peripheral lymph node addressin molecule (PNAd), which would allow immune cells to home to these sites from the blood stream (data not shown). Using image analysis, we determined that the area within the aggregate covered by vessels (ie, inside the hatched box in Figure 1D) was 37.8 ± 1.1% compared with 9.5 ± 0.74% in the surrounding omental tissue (ie, outside the hatched box in Figure 1D), a greater than fourfold difference (Figure 1F). Although unproven, this increased vascular area is consistent with an active physiological process to support the abundant immune cells found within the aggregates.

Tumor Growth on Immune Aggregates

We next examined the time course of tumor growth and determined how it affected the organized structure and vasculature of the omental immune aggregates. Three-color fluorescence whole mount histology was used to monitor the growth kinetics of B16/GFP and the morphology of the existing immune cell architecture and vasculature. B16/GFP cells were injected intraperitoneally, and omenta were removed after 2, 4, 6, or 8 days and stained with anti-CD45 antibody to label immune cells and anti-CD31 to mark blood vessels. Images in Figure 2 are representative of omental immune aggregates from each time point showing immune cells (red, top panels), an overlay of bound tumor cells and immune cells (green and red, middle panels), and blood vessels (yellow, bottom panels). At day 2, low numbers of tumor cells were visible bound to the aggregates, which exhibited the distinct vascular bed associated with these structures as shown in Figure 1. Abundant tumor growth was evident

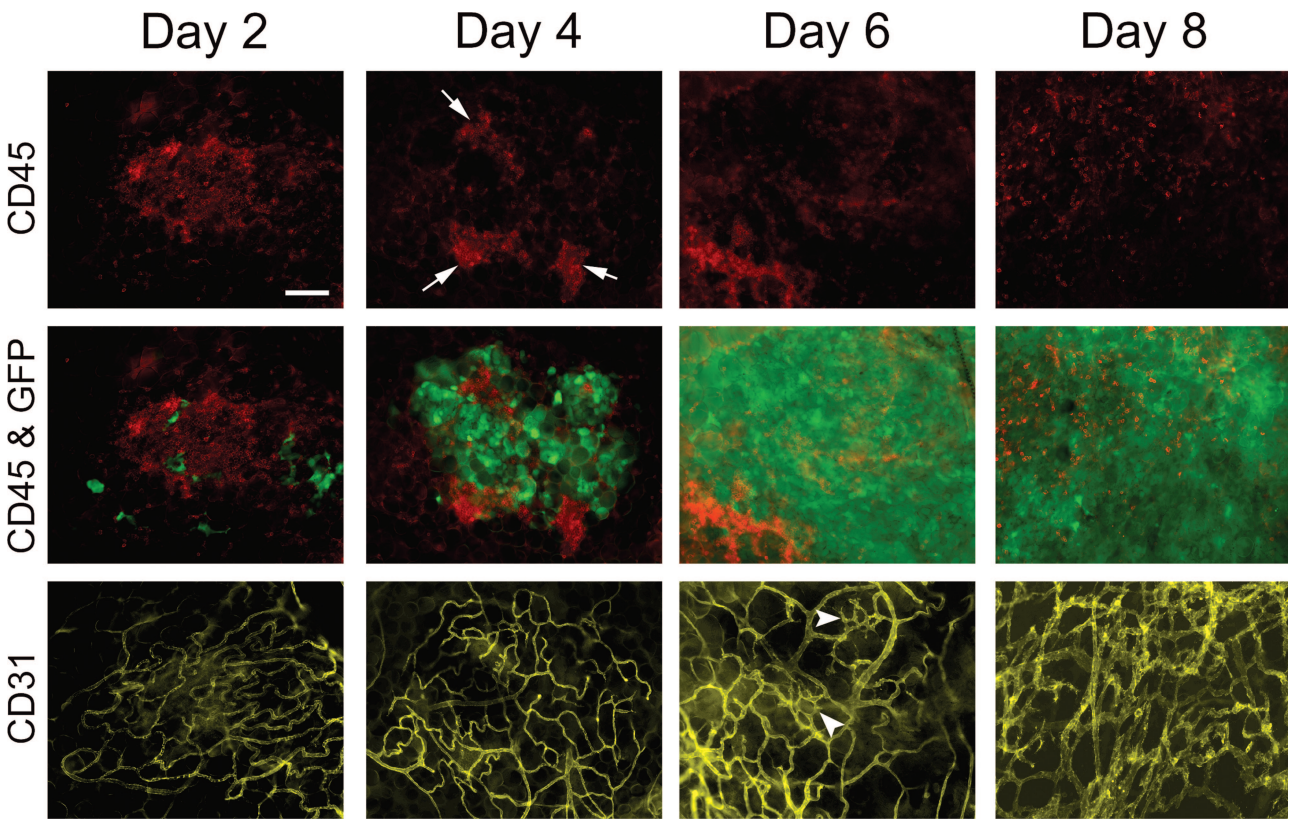

Figure 2. Tumor cells infiltrate immune aggregates and exhibit rapid growth. B16/GFP tumor cells (1×10^5) were injected intraperitoneally into mice. On the indicated days, omenta were removed and stained simultaneously with anti-CD45 to label immune cells (red) and anti-CD31 to mark blood vasculature (yellow) and visualized in separate fluorescence channels using whole mount microscopy. Images of the same field of view were taken on each day for immune cells alone (top), immune cells and GFP^+ tumor cells shown as an overlay (middle), or blood vessels alone (bottom). Representative images from three separate experiments from each day are depicted. **Arrowheads** show morphological changes indicative of angiogenesis. Scale bar = 100 μm.

on day 4, whereas the structure of the immune cell clusters was disrupted leaving segmented groups of cells (arrows) located nearer to the outer perimeter of the vascular bed. Only small groups of immune cells remained on day 6 along with evidence of sprouting and webbed vessels indicative of angiogenesis (arrowheads).[31,32] By day 8, tumor growth had completely displaced most of the immune cells except for sporadic $CD45^+$ cells found within the tumor mass, which are possibly remnants of the original immune aggregate. In addition, at this time point the vasculature had taken on the typical chaotic, dense morphology commonly associated with aggressive angiogenesis in tumors.[21]

The Unique Phenotype of the Blood Vasculature of the Omentum May Contribute to Tumor Growth

Our finding that tumor cells not only attached preferentially to the areas of the omentum containing immune aggregates but also grew aggressively led us to hypothesize that the vasculature in these areas may be especially conducive to supporting cell growth. To obtain an overview of the molecules expressed within the naïve omentum that might contribute to this phenotype, we performed a preliminary gene array examining 96 genes commonly associated with cell adhesion and the angiogenesis process (data not shown). We found high expression of genes that induce angiogenesis as well as those that could be considered as anti-angiogenic, a balance consistent with tissues that exhibit vascular quiescence.[22] However, despite the usefulness of such arrays in providing an overview of the genes expressed by the tissue, they were unable to provide information on localized expression, the relative importance of individual molecules, or even if the protein is being produced. For this reason, we decided to narrow our focus and examine the protein expression of a few molecules in more detail, concentrating on expression within the area of the immune aggregates, because these areas are the main sites of tumor cell attachment and growth.

Based on the gene array, CD105, a proliferation-associated antigen located predominately on endothelial cells undergoing active angiogenesis,[33,34] was moderately expressed on the omentum. Fluorescence microscopy was used to determine whether this molecule was up-regulated on the vasculature within the immune aggregates. Figure 3 depicts an immune aggregate (Figure 3A, red and outlined in white), along with its associated blood vessels (Figure 3B, green), which stained positively for CD105 (Figure 3C, orange as a result of the overlay of blood vessels and CD105 staining), whereas vasculature outside of the aggregate was low or negative for CD105 expression (arrows). This suggests that the vessels within

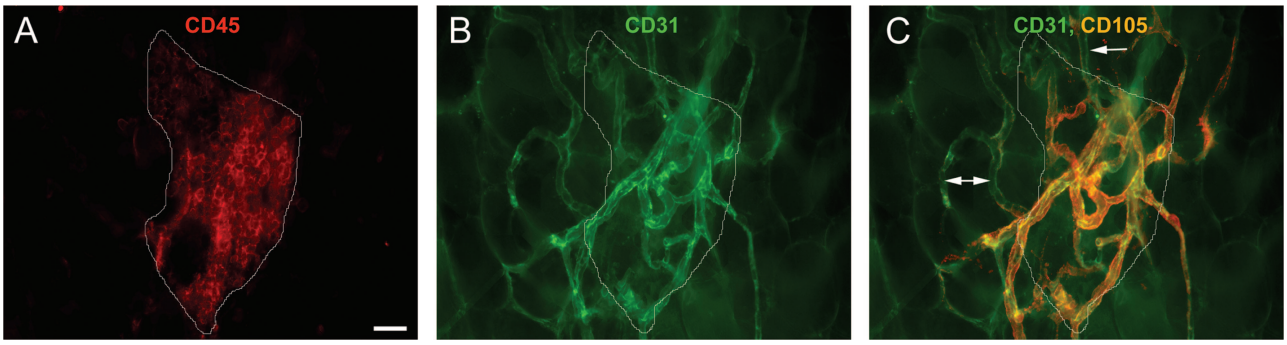

Figure 3. Vasculature within the immune aggregates specifically expresses the proangiogenic molecule CD105. **A–C:** Omenta were removed and stained simultaneously with anti-CD45 to label immune cells (red) (**A**), anti-CD31 to identify blood vessels (green) (**B**), and anti-CD105 (orange) shown as an overlay on blood vessels (**C**). An outline (white line) of the boundary of immune cells from **A** is also illustrated in **B** and **C**. Vessels outside of the aggregate were low or negative for CD105 expression (**arrows**). Images are representative of four independent experiments. Scale bar = 25 μm.

the immune aggregates are in a proangiogenic state distinct from the vessels in the surrounding tissue.

To confirm this conclusion we sought further evidence of an active process of angiogenesis. It has been reported that during the early stages of neovascularization, leading sprouts consisting of collagen IV basement membrane can be observed before endothelial cell proliferation and migration.[35–37] To determine whether these sprouts existed in the omentum, immune aggregates and their associated vasculature were identified as before (Figure 4A, overlay of immune cells in red, and blood vessels in green) and stained simultaneously with anti-collagen IV to highlight sprouts (Figure 4, B and C). In Figure 4B, collagen is observed sheathing most vessels in the aggregate. Multiple sprouts can also be identified in this image (arrows), most residing to the outside boundary of the aggregate vasculature. A magnified image of the hatched box (Figure 4C) illustrates that these structures possessed distinct sprout morphology. No sprouts were detected in areas outside of the immune aggregates. A different area containing a developing vessel was stained simultaneously with collagen IV (Figure 4D, red) and CD31 to detect endothelial cells (Figure 4E, green), and both images are shown as an overlay in Figure 4F. The collagen IV-positive sprout was traced in Figure 4D and copied into Figure 4E, illustrating that few to no CD31-expressing endothelial cells could be observed within this collagen sprout at this time. Analysis of multiple sprouts revealed this to be a common pattern; however, in some cases small processes with $CD31^+$ cells within them were found, and these also stained positively with CD105 (data not shown). The number of

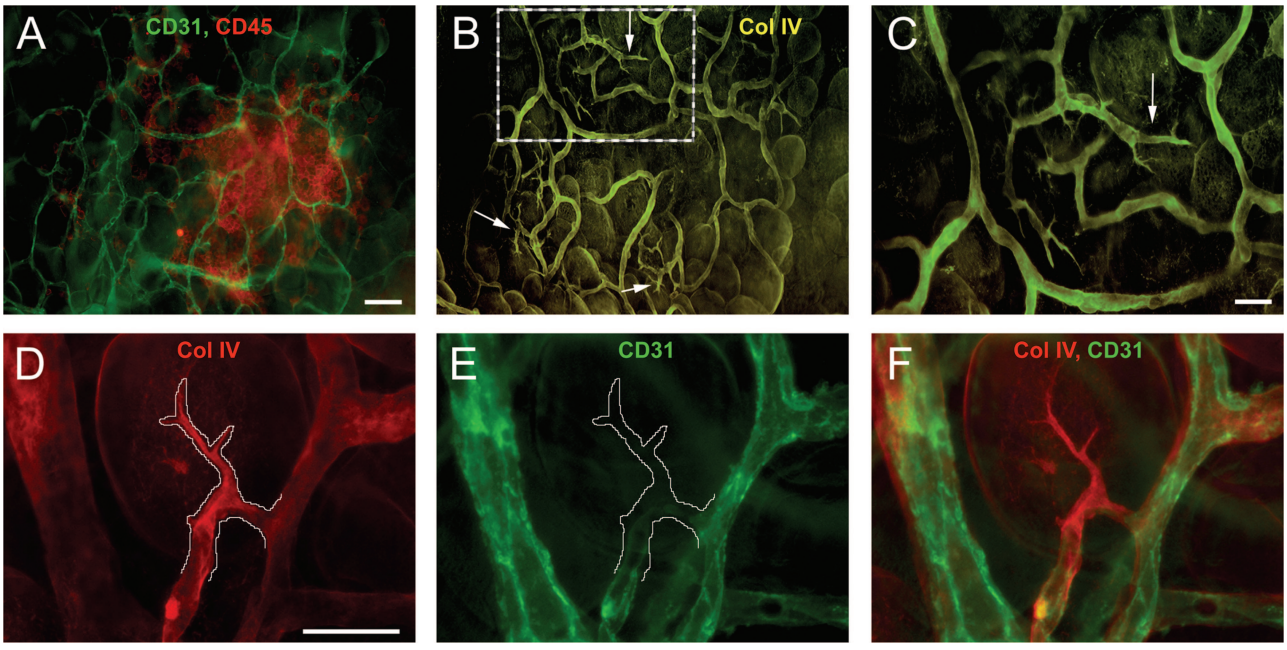

Figure 4. Definitive vascular sprouting can be observed within omental immune aggregates from naïve mice. **A:** Omenta were stained with anti-CD45 (red) or anti-CD31 (green) to demonstrate a typical immune aggregate consisting of immune cells and blood vessels, respectively. **B:** The same field of view stained simultaneously with anti-collagen type IV (yellow) identifying vascular sprouts near the boundaries of the aggregate vasculature (**arrows**). **C:** Higher magnification of the inset in **B**. In a separate immune aggregate, a more detailed examination of the vascular sprouts was performed on the same field of view in images **D** to **F**, illustrating anti-collagen type IV (red) staining with the sprout outlined (**D**), blood vessels lacking CD31 reactivity in the area of the sprout (white line) (**E**), and an overlay of both images (**F**). Images are representative from six independent experiments. Scale bars: 50 μm (**A**, **B**); 25 μm (**C–F**).

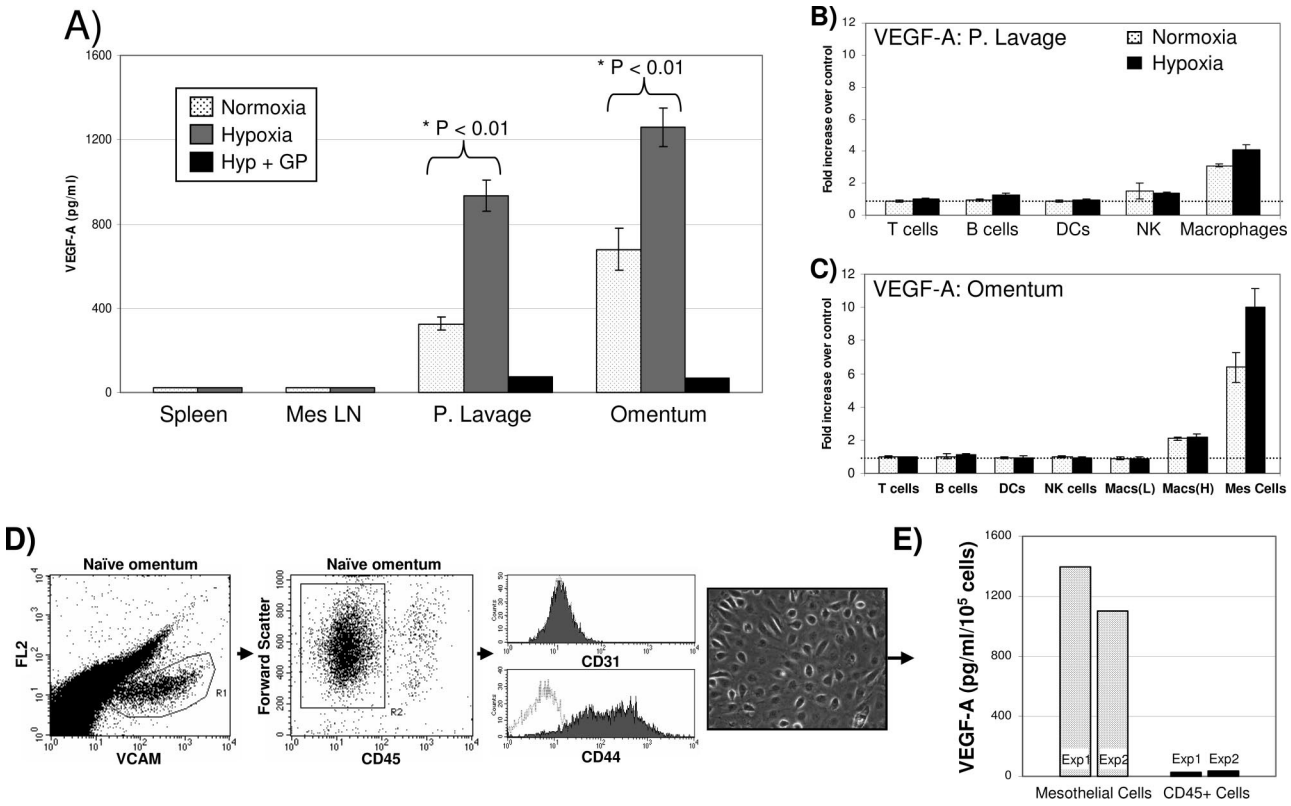

Figure 5. VEGF-A production by cell types found within the omentum or peritoneal cavity. **A:** Cells (1×10^6) from the spleen, mesenteric LN, peritoneal lavage, or omentum were incubated in normoxic, hypoxic, or hypoxic plus brefeldin A (Golgi Plug, +GP) conditions for 16 hours, and VEGF-A in the supernatant was measured by ELISA. Subsets of cells from either the peritoneal cavity (**B**) or the omentum (**C**) were tested for VEGF-A production using intracellular staining and reported as the fold increase over controls as described in Materials and Methods. Cells not producing VEGF-A would have a fold increase of 1 (dotted line). Macrophages from the omentum were divided into those expressing low [Macs (L)] or high [Macs (H)] levels of F4/80. **D:** Phenotypic and morphological analysis of mesothelial cells isolated from single cell suspensions of the omentum. Gating on a population of $VCAM^+$ cells (left dot plot) revealed this to be $CD45^-$ (middle dot plot). Further analysis of this $VCAM^+$, $CD45^-$ population demonstrated the cells were $CD31^-$ (top histogram), and $CD44^+$ (bottom histogram). The digital image is representative of these cells when grown *in vitro* after isolation by FACS (see below) showing a cobblestone morphology, which is typical of mesothelial cells. **E:** Mesothelial cells or $CD45^+$ immune cells were sorted using flow cytometry and cultured in normoxic conditions, and VEGF-A production was measured after 16 hours of incubation as above. Each experiment described above was repeated at least three times with the exception of the sorted cells, which was done twice. Statistical significance was determined using a one-way analysis of variance followed by Bonferroni's multiple comparison test.

sprouts in naïve mice was enumerated by image analysis as described in Materials and Methods. We determined that ~5 ± 0.44 sprouts were found per average-size immune aggregate, with 80 ± 1% of all immune aggregates analyzed possessing distinct sprout structures. These results are consistent with the conclusion that most of the immune aggregates of the naïve omentum have vasculature in an angiogenic state, which does not occur in the other parts of the omentum.

Cellular Source of VEGF-A Production from Omental Immune Aggregates

The constitutive angiogenic state of the vasculature found within the aggregates is unusual for a normal tissue, so we addressed what cell type was responsible and the mechanisms involved in this induction. The gene array of the omentum had indicated that VEGF-A, a known potent initiator of angiogenesis and vascular sprout formation[38,39] was expressed at a relatively low level in the context of the entire omentum (data not shown). We first examined the VEGF-A production from single-cell suspensions of the omentum, which contained predominately immune cells including macrophages, which are known to express VEGF. As additional controls, other tissues composed primarily of immune cells including cells obtained from the peritoneal cavity by lavage, from spleen, and from mesenteric lymph nodes were also examined for VEGF-A production. These cell populations were incubated for 16 hours under normoxic conditions (21% atmospheric oxygen), and VEGF-A production assessed by ELISA. Under such normal physiological oxygen conditions, omental cells produced more VEGF-A than peritoneal lavage cells, suggesting a constitutive production of this molecule (Figure 5A). Production of VEGF-A is induced by hypoxia, as might occur during tumor growth in a local microenvironment. As expected, incubation of both peritoneal lavage and omental cell populations under severe hypoxic conditions (<0.01% oxygen) increased the level of VEGF-A in the culture supernatants. No VEGF-A was detected in the primarily lymphoid splenic and lymph node preparations.

To define the cell type responsible for VEGF-A secretion, intracellular staining and flow cytometry were used as detailed in Materials and Methods. Peritoneal lavage and omental cell preparations were treated with brefeldin

A (Golgi Plug, +GP), which effectively sequestered the VEGF-A intracellularly (Figure 5A). The mean fluorescence intensity of VEGF-A from specific immune subsets treated with brefeldin A in normoxic or hypoxic conditions was compared with the mean fluorescent intensity of cells without brefeldin A (serving as a negative control because all VEGF-A actively being produced would be secreted) and expressed as fold increase. This analysis was performed on both peritoneal lavage (Figure 5B) and omental cells (Figure 5C). In the lavage, macrophages, which are primarily mature F4/80^{hi} cells, were the major immune cell type that actively produced VEGF-A. This is in agreement with published literature on peritoneal macrophages.[40,41] Interestingly, omental immune cells produced no detectable levels of VEGF-A except for a small population of F4/80^{hi} macrophages (which represented 24% of all omental macrophages), whose production was only twofold greater than the negative control. However, within the omental cells we commonly found a non-CD45 population that stained significantly more positive for intracellular VEGF-A. The cell surface phenotype (VCAM$^+$, CD44$^+$, CD45$^-$, CD31$^-$) and the cobblestone morphology they exhibited when grown in culture (Figure 5D) are consistent with the published characteristics of mesothelial cells.[42–44] When analyzed for intracellular VEGF-A, 25 $\pm$ 1.3% of the mesothelial cells demonstrated a 6.4-fold increase over controls under normoxic conditions (Figure 5C). Hypoxia increased this population to 39 $\pm$ 3.9% and further induced VEGF-A production to 10-fold greater than controls ($P < 0.05$).

To confirm that mesothelial cells were responsible for most of the VEGF-A production in Figure 5A, we simultaneously sorted CD45$-$VCAM-1$^+$ mesothelial cells and CD45$^+$ cells into separate populations. These cells were cultured as described above, and the amount of VEGF in the culture supernatant determined by ELISA. This experiment was repeated twice with similar results (Figure 5E) and demonstrates that sorted omental mesothelial cells produced 100-fold more VEGF-A on a per cell basis compared with the CD45$^+$ immune cells alone in normoxic conditions. These mesothelial cells, which comprised 5% of the total omental cells, were responsible for 85% of the VEGF-A produced by the total omental population. From these results, we concluded that omental mesothelial cells are responsible for the majority of VEGF-A produced, and this level is augmented under hypoxic conditions.

Hypoxia Analysis of Omental Cell Types

Suboptimal levels of oxygen (hypoxia) can cause the induction of VEGF-A through the binding of hypoxia inducible factor-1 (HIF-1α) to the hypoxia response element within the VEGF promotor.[41,45] Therefore, it was likely that some cells may be producing VEGF-A in response to conditions of low oxygen within the immune aggregate. To determine whether a specific population of cells was hypoxic, mice were injected with EF5, a pentafluorinated derivative of etanidazole, which forms covalent adducts with intracellular proteins under conditions of low oxygen tension.[46] A fluorophore-labeled monoclonal antibody, ELK3-51, specific for the metabolite was used to detect hypoxic cells.[47] Specific cell populations of the omentum were then examined for hypoxic fractions using flow cytometry (Figure 6). A proportion of the F4/80$^+$ macrophages (Figure 6A, middle histogram) and the mesothelial cells (bottom histogram) stained positively with ELK3-51 over no drug controls. Interestingly, the hypoxic fraction of both populations (25% macrophages, 28% mesothelial cells) (Figure 6B) was similar to the percentage of constitutive VEGF-A-producing cells, respectively (24% macrophages, 25% mesothelial cells). Only minimal hypoxic fractions (3%) were observed in the remaining immune cells, which constitute predominately lymphocytes (top histogram). This data led us to conclude that a portion of the macrophages, and even more importantly the mesothelial cells found within the immune aggregates, exhibited some level of hypoxia potentially triggering the induction of VEGF-A in these cells.

Orientation of the Mesothelial Cells on Omental Immune Aggregates

Our data in Figure 5 suggest that mesothelial cells secrete abundant amounts of VEGF-A, which is further increased by hypoxic conditions. Because a quarter of these cells from the omentum are constitutively hypoxic, it is possible that these cells reside on immune aggregates, thereby potentiating the induction of angiogenesis. Based on a preliminary gene array indication of high expression levels of the adhesion molecule VCAM-1 (data not shown) and the reported expression of VCAM-1 by mesothelial cells, we decided to use anti-VCAM-1 to determine the location of mesothelial cells within the omentum. VCAM-1$^+$ mesothelial cells are observed (Figure 7A, red) in a patchy pattern, that appear to blanket the cluster of CD45$^+$ immune cells (green), which generally lie central to the mesothelial cells [Figure 7B, overlay of mesothelial cells (red) and immune cells (green)]. VCAM$^+$ mesothelial cells were only found on immune aggregates on the omentum. Interestingly, the outer boundary of the mesothelial cells (white line) on each aggregate coincided with the outer boundary of the aggregate vasculature [Figure 7C, overlay of vessels (red) and immune cells], suggesting that these cells may regulate vascular growth within the aggregates. Closer examination of this VCAM$^+$ population revealed large cells that possessed a typical cobblestone morphology commonly associated with mesothelial cells from the peritoneal cavity (Figure 7D). Confocal microscopy of the immune aggregates (Figure 7E) revealed that the orientation of VCAM$^+$ mesothelial cells (arrows, orange) was above the CD45$^+$ immune cells (green) based on descending optical slices through the omentum. Therefore, mesothelial cells were found to cover both the immune cells and blood vessels found in each aggregate.

Discussion

Formation of initial metastases from intra-abdominal malignancies such as stomach, pancreas, ovarian, and co-

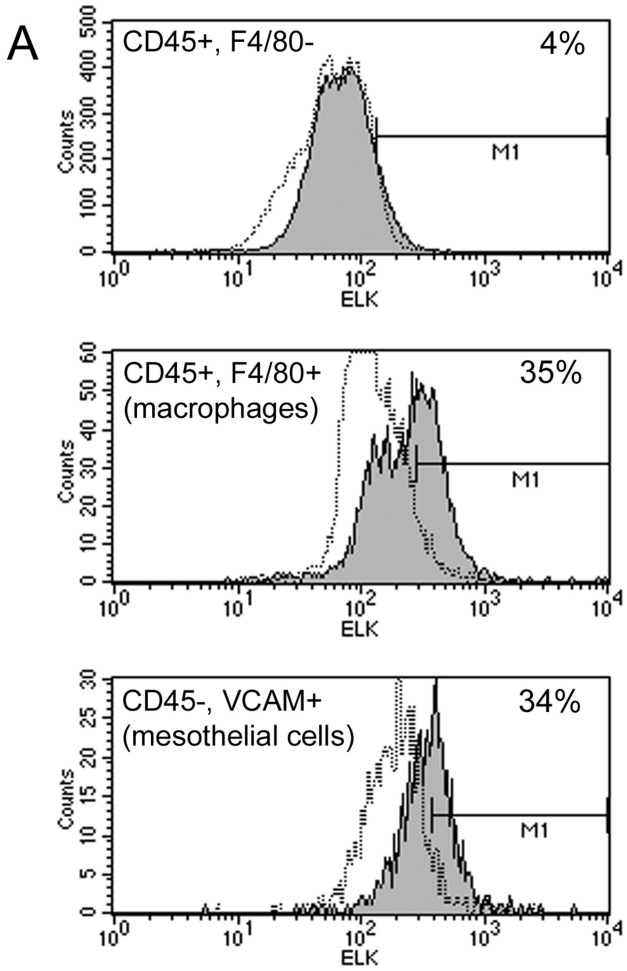

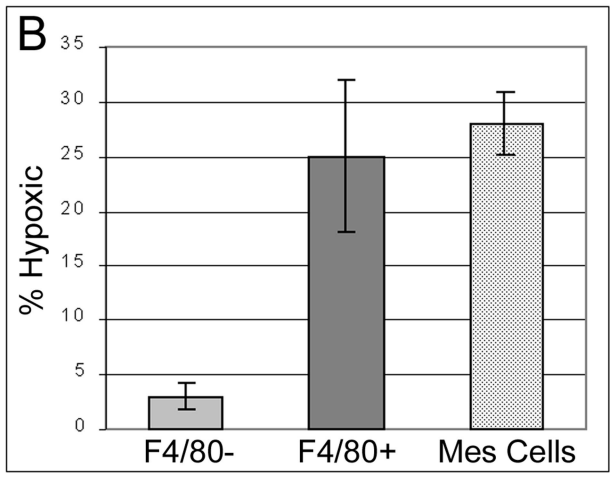

Figure 6. Macrophages and mesothelial cells stain positively for the hypoxic marker EF5. Omental single-cell suspensions were obtained from mice treated with EF5 and stained with surface markers for macrophages ($CD45^+$, $F4/80^+$), mesothelial cells ($CD45^-$, $VCAM^+$), and EF5 (ELK 3.51). Hypoxic fractions (shaded) were defined as the percent positive over no drug controls (dotted lines). **A:** Representative histograms are shown. **B:** Arithmetic means and SEM were calculated for each subset based on five ($F4/80^-$ and $F4/80^+$ populations) or three (mesothelial cells) independent experiments. The percentage of hypoxic cells in the $CD45^+$, $F4/80^-$ population is significantly different from both the $CD45^+$, $F4/80^+$ population and the mesothelial cells with $P < 0.05$ as determined by analysis of variance and Bonferroni's multiple comparison test.

lon primarily occurs within the peritoneal cavity by direct seeding of metastatic cells onto peritoneal surfaces. As we have shown in this report and as observed by others,[7,48] these metastatic foci have a very distinct growth pattern. Two factors contribute to the unique growth characteristics of intraperitoneal metastases. First, the tumor cells attach preferentially to aggregates of immune cells, which are found in greatest number on the omentum but also on the mesentery and adipose tissue proximal to the female reproductive tract (data not shown). This attachment occurs rapidly, as small tumor foci are visible as early as 1 hour after intraperitoneal injection of tumor cells. This attachment has been observed for numerous cell lines in our study and is consistent with other investigations indicating that it occurs in diverse species including mice, rats, and humans.[6,7] The mechanisms responsible for the specific attachment remain to be determined. It is not clear whether the known filtering capacity of the immune aggregates[49] is involved in the attachment process or whether specific receptor/ligand pairs are required. If specific receptors play a role, they must be ones that are widely expressed on many cell types. Although the mechanism of the attachment process per se was not the primary focus of the current article, our preliminary confocal studies indicate that the injected tumor cells bind above the immune cells (data not shown), perhaps to the mesothelial cells or the extracellular matrix. This important process will be studied further in future experiments.

The second factor that may contribute to metastatic foci is the unique characteristics of the vasculature within the regions of the immune aggregates. We have determined that the density of blood vessels within these areas is four times greater than that in the surrounding omental tissue. Furthermore, these vessels in omenta from naïve mice appear to be constitutively angiogenic, perhaps ready to support the rapid influx of immune cells that occurs when pathogens are present within the peritoneal cavity. This is particularly noteworthy because most blood vessels within a normal individual are quiescent, with only 0.01% of all endothelial cells actively dividing.[31] Thus, these sites may be areas of particularly fertile soil for the growth of metastatic tumor cells.

Initial studies from Judah Folkman[50] in the early 1970s first described how tumor progression was dependent on angiogenesis. This concept was further supported and is now widely accepted based on numerous studies highlighting the necessity of new vessel growth for both primary and metastatic tumor growth. However, metastatic tumor cells must survive

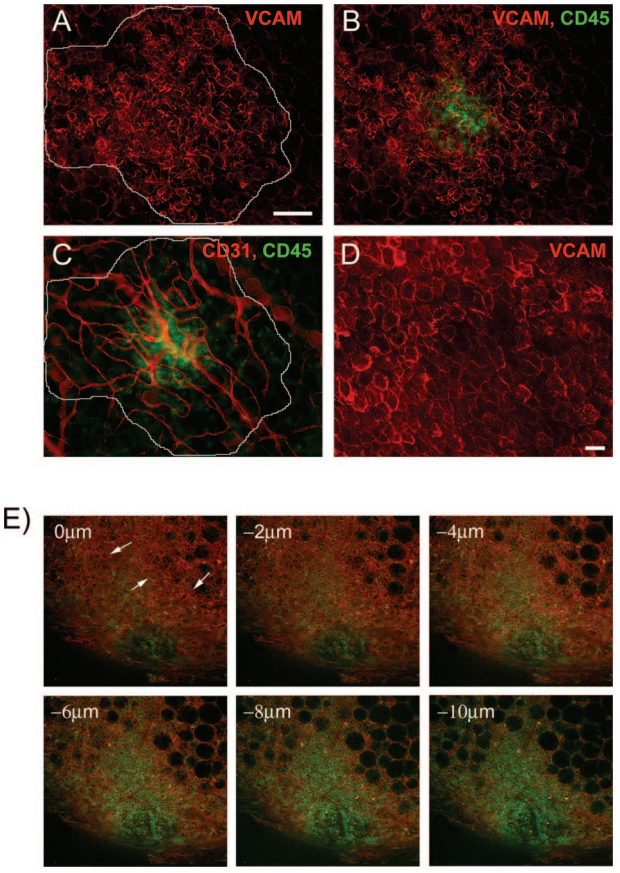

Figure 7. VCAM$^+$ mesothelial cells have a defined patchy architecture over the immune aggregate. Mesothelial cells were identified within immune aggregates using anti-VCAM (red) (**A**), and their outer boundary was traced. In **B**, immune cells labeled with anti-CD45 (green) and mesothelial cells (red) are shown as an overlay. **C:** Within the same field of view, immune cells and blood vessels labeled with anti-CD31 (red) are shown as an overlay with the boundary of the mesothelial cells shown in white. **D:** A higher magnification of mesothelial cells from a different immune aggregate illustrating large, cobblestone-like cells. **E:** Confocal analysis of an immune aggregate stained for immune cells (green) and mesothelial cells (orange). Descending confocal slices (0 to 10 μm) of the immune aggregate with mesothelial cells (**arrows**) visible near the top of the aggregate. Conventional microscopy experiments were repeated three times, whereas confocal experiments were preformed twice. Scale bars: 100 μm (**A–C**); 25 μm (**D**).

before the induction of new vessel growth, and thus, attachment to sites rich in vessels may facilitate the initial growth. One mechanism proposed is vessel co-option, in which metastatic cells draw oxygen and nutrients from existing vasculature without inducing new vessels.[17,26] Our data would suggest that metastatic cells do indeed initially co-opt vessels within the omental immune aggregate, and it is this co-option that promotes early tumor survival. An earlier report suggested a mechanism in which tumor cells may initially co-opt vessels; however, abundant tumor growth in the absence of compensatory angiogenesis can cause regression of the existing vasculature.[32,51] This regression may be accompanied by massive tumor cell loss induced by hypoxia and apoptosis, resulting in the secretion of proangiogenic factors, which in turn initiate aggressive angiogenesis.[17,32] Even though we observed tumor co-option of vessels, abundant vessel regression was not detected before the onset of angiogenesis. One possibility is that the regression observed in other studies occurred because the vessels were quiescent and not readily inducible. In contrast, the vasculature within the immune aggregates appears to be constitutively in a state of readiness to expand, and therefore, no lag phase would be present. Interestingly, gene array analysis of the naïve omentum revealed high expression of both pro- and antiangiogenic genes. Despite the apparent balance between these genes in the overall omentum, as would be expected in normal tissue,[22] there was also expression of the potent angiogenic gene VEGF-A. VCAM$^+$ mesothelial cells were determined to be the chief producers of VEGF-A within the omentum, and these cells were found predominately on immune aggregates. This is indirect evidence that these cells and the potent proangiogenic factor they secrete, VEGF-A, may play a role in the apparent induction of angiogenesis within immune aggregates as evidenced by the expression of CD105 and the presence of vascular sprouts in these areas.

Our studies examined VEGF-A production by various cell types from the omentum, including immune cells and mesothelial cells; however, our isolation technique excluded omental adipocytes from the analysis. A previous study reported the production of VEGF-A from isolated rat omental adipocytes and suggested that these cells may play a role in omental-mediated angiogenesis.[52] This report made no mention of immune aggregates or vasculature associated with these structures. Although adipocytes may secrete VEGF-A, the localization of angiogenesis to the immune aggregates that we have observed is inconsistent with adipocytes, which are found throughout the omentum, being the major inducers of vessel formation at these sites. In addition, the basic architecture of the immune aggregate is such that immune cells infiltrated by blood vessels lie atop of adipocytes. Because vessel growth is in the direction of a proangiogenic gradient, it is more conceivable that cells above the aggregate secrete the factors causing vessels to grow throughout the structure. If adipocytes secreted proangiogenic factors, vessel growth would be directed downward and away from the aggregate. It is more likely that omental adipocytes act as energy depots, secreting fatty acids or glutamine that lymphoid cells may use during proliferation.[53]

Mesothelial cells form a monolayer throughout most of the peritoneal cavity serving as a protective nonadhesive barrier for serosal surfaces and internal organs.[54] More recently, additional functions have been attributed to these cells, one being the ability to secrete various proinflammatory cytokines and chemokines in response to peritoneal infections.[54–56] In our study, VCAM$^+$ mesothelial cells were localized to immune aggregates on the omentum and were able to secrete abundant amounts of VEGF-A, which was augmented by hypoxia. However, other studies have demonstrated that mesothelial cell production of VEGF-A can also be triggered by TGF-β and by bacterial pathogens.[57,58] This would suggest that additional factors that may be present during a peritoneal immune response, along with hypoxia, could stimulate

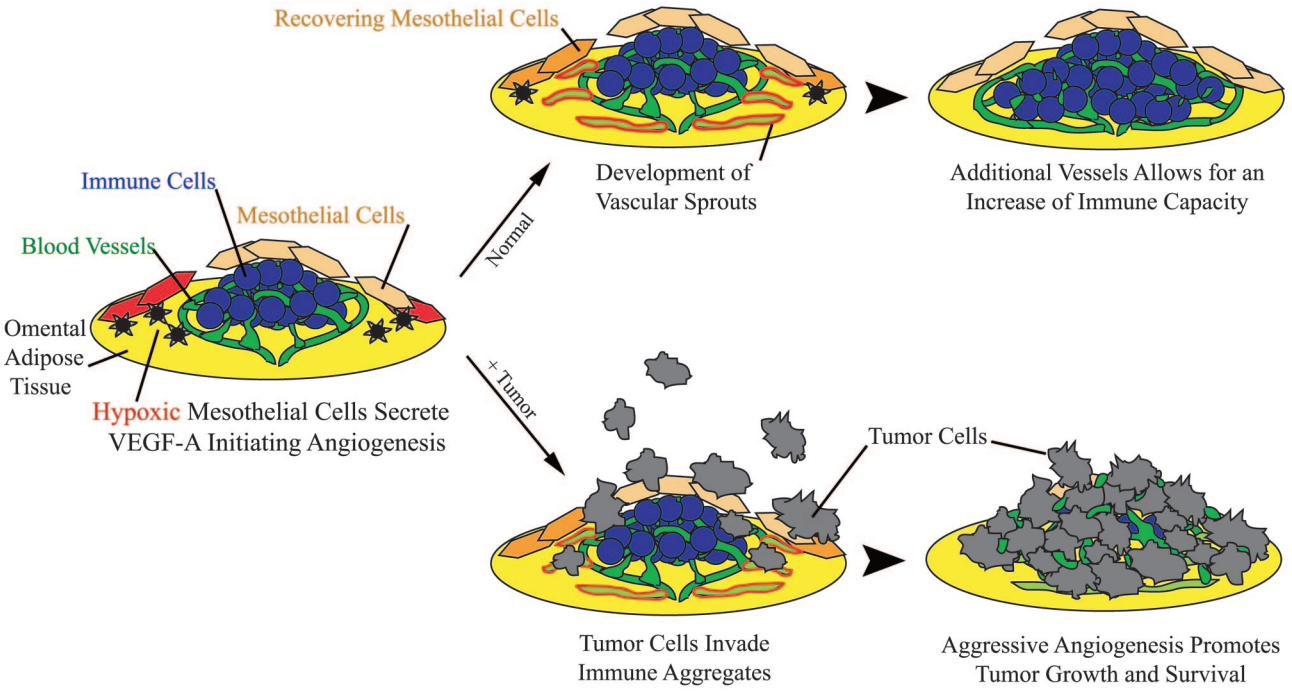

Figure 8. Proposed model. As described, omental immune aggregates contain mesothelial cells, some of which are hypoxic (red) and therefore secrete VEGF-A (**black asterisks**). In a normal physiological setting (top), VEGF-A production can stimulate blood vessels to produce vascular sprouts (green outlined in red), resulting in the induction of angiogenesis and recovery of once-hypoxic mesothelial cells. The increase of vessels delivers more immune cells, along with additional oxygen and nutrients necessary to support the influx of cells. In a metastasis model (bottom), tumor cells invade aggregates and co-opt the existing dense vasculature. Because angiogenesis is already induced, new blood vessel formation is rapid, resulting in aggressive tumor growth.

mesothelial cells associated with omental immune aggregates to secrete proangiogenic molecules. Interestingly, these cells express adhesion molecules that may mediate the attachment of immune and, more importantly, malignant cells within the peritoneal cavity and therefore may promote the spread of metastatic disease.[43,59–61] However, it remains to be shown whether mesothelial cells on the immune aggregates are responsible for the selective binding of tumor and immune cells to these sites.

A conceptual framework for our findings is illustrated in Figure 8. A simplified example of an omental immune aggregate is shown as a slightly raised mound of cells resting on a layer of adipocytes. It consists of a cluster of immune cells infiltrated with a dense network of capillaries, covered by a porous layer of mesothelial cells that are exclusive to the aggregates (Figure 8, left). Our results indicate that a portion (25%) of these mesothelial cells are hypoxic on removal from naive omenta, suggesting that these hypoxic cells may be associated with immune aggregates in a normal physiological setting. A similar proportion of these cells were found to secrete elevated amounts of VEGF-A, and it is tempting to speculate that these are the same population, but further experimentation will be needed to test this possibility. The exact role these cells play is unclear; however, one possibility is that mesothelial cells regulate the formation of new blood vessels within the aggregates, ultimately controlling the size of these structures. For example, in response to a pathogenic stimulus, an influx of immune cells into the immune aggregates may create a hypoxic microenvironment triggering the mesothelial cells on the aggregates to secrete VEGF-A. Nearby capillaries within the existing aggregate would be stimulated by VEGF-A, and grow in the direction of the VEGF-A gradient (Figure 8, top middle). This would not only allow vessels to deliver oxygen to hypoxic areas, but the resultant vasculature may express PNAd and therefore allow additional immune cells to home from the bloodstream into the once vacant areas of the aggregate. Ultimately, the increase of vasculature could support the expansion or influx of immune cells needed in the response to peritoneal infections (Figure 8, top right).

In our metastasis model (Figure 8, bottom), single tumor cells selectively invade the immune aggregates, which already exhibit a fourfold greater vascular area than the surrounding omental tissue. This rich network of vessels may provide tumor cells with necessary factors required for early survival; however, tumor progression requires the induction of new blood vessels from once quiescent ones. This process is commonly referred to as the angiogenic switch and can often be the limiting factor determining whether or not malignant cells survive. Because our data suggest that the angiogenic switch is already turned on in the aggregates, this may facilitate tumor growth resulting in large clusters of tumor cells (Figure 8, bottom right). Thus, the microenvironment of the immune aggregate's default is in favor of angiogenesis and therefore supports metastatic survival and immediate tumor growth.

References

1. Mahteme H, Hansson J, Berglund A, Pahlman L, Glimelius B, Nygren P, Graf W: Improved survival in patients with peritoneal metastases from colorectal cancer: a preliminary study. Br J Cancer 2004, 90:403–407
2. Healy JC, Reznek RH: The peritoneum, mesenteries and omenta: normal anatomy and pathological processes. Eur Radiol 1998, 8:886–900
3. Buy JN, Moss AA, Ghossain MA, Sciot C, Malbec L, Vadrot D, Paniel BJ, Decroix Y: Peritoneal implants from ovarian tumors: CT findings. Radiology 1988, 169:691–694
4. Sheth S, Horton KM, Garland MR, Fishman EK: Mesenteric neoplasms: CT appearances of primary and secondary tumors and differential diagnosis. Radiographics 2003, 23:435–473
5. Lawrance RJ, Loizidou M, Cooper AJ, Alexander P, Taylor I: Importance of the omentum in the development of intra-abdominal metastases. Br J Surg 1991, 78:117–119
6. Krist LF, Kerremans M, Broekhuis-Fluitsma DM, Eestermans IL, Meyer S, Beelen RH: Milky spots in the greater omentum are predominant sites of local tumour cell proliferation and accumulation in the peritoneal cavity. Cancer Immunol Immunother 1998, 47:205–212
7. Hagiwara A, Takahashi T, Sawai K, Taniguchi H, Shimotsuma M, Okano S, Sakakura C, Tsujimoto H, Osaki K, Sasaki S: Milky spots as the implantation site for malignant cells in peritoneal dissemination in mice. Cancer Res 1993, 53:687–692
8. Dullens HF, Rademakers LH, Doffemont M, Van Veen PT, Bulder R, Den Otter W: Involvement of the omental lymphoid organ in the induction of peritoneal immunity against tumor cells. Invasion Metastasis 1993, 13:267–276
9. Van Vugt E, Van Rijthoven EA, Kamperdijk EW, Beelen RH: Omental milky spots in the local immune response in the peritoneal cavity of rats. Anat Rec 1996, 244:235–245
10. Krist LF, Eestermans IL, Steenbergen JJ, Hoefsmit EC, Cuesta MA, Meyer S, Beelen RH: Cellular composition of milky spots in the human greater omentum: an immunochemical and ultrastructural study. Anat Rec 1995, 241:163–174
11. Beelen RH: The greater omentum: physiology and immunological concepts. Neth J Surg 1991, 43:145–149
12. Ranvier L: Du development et de l'accroisement des vaisseux sanguins. Arch Physiol 1874, 1:429–450
13. Dux K, Rouse RV, Kyewski B: Composition of the lymphoid cell populations from omental milky spots during the immune response in C57BL/Ka mice. Eur J Immunol 1986, 16:1029–1032
14. Beelen RH, Fluitsma DM, Hoefsmit EC: The cellular composition of omentum milky spots and the ultrastructure of milky spot macrophages and reticulum cells. J Reticuloendothel Soc 1980, 28:585–599
15. Funda D, Holub M, Sykora V: Development of the cellular response in the mouse omentum after intraperitoneal immunization. APMIS 1993, 101:939–945
16. Ansel KM, Harris RB, Cyster JG: CXCL13 is required for B1 cell homing, natural antibody production, and body cavity immunity. Immunity 2002, 16:67–76
17. Kirsch M, Schackert G, Black PM: Metastasis and angiogenesis. Cancer Treat Res 2004, 117:285–304
18. Wijffels JF, Hendrickx RJ, Steenbergen JJ, Eestermans IL, Beelen RH: Milky spots in the mouse omentum may play an important role in the origin of peritoneal macrophages. Res Immunol 1992, 143:401–409
19. Shimotsuma M, Shields JW, Simpson-Morgan MW, Sakuyama A, Shirasu M, Hagiwara A, Takahashi T: Morpho-physiological function and role of omental milky spots as omentum-associated lymphoid tissue (OALT) in the peritoneal cavity. Lymphology 1993, 26:90–101
20. Koenen HJ, Smit MJ, Simmelink MM, Schuurman B, Beelen RH, Meijer S: Effect of intraperitoneal administration of granulocyte/macrophage-colony-stimulating factor in rats on omental milky-spot composition and tumoricidal activity in vivo and in vitro. Cancer Immunol Immunother 1996, 42:310–316
21. Zetter BR: Angiogenesis and tumor metastasis. Annu Rev Med 1998, 49:407–424
22. Folkman J: Role of angiogenesis in tumor growth and metastasis. Semin Oncol 2002, 29:15–18
23. Dvorak HF, Brown LF, Detmar M, Dvorak AM: Vascular permeability factor/vascular endothelial growth factor, microvascular hyperpermeability, and angiogenesis. Am J Pathol 1995, 146:1029–1039
24. Ellis LM, Fidler IJ: Angiogenesis and metastasis. Eur J Cancer 1996, 32A:2451–2460
25. Li CY, Shan S, Huang Q, Braun RD, Lanzen J, Hu K, Lin P, Dewhirst MW: Initial stages of tumor cell-induced angiogenesis: evaluation via skin window chambers in rodent models. J Natl Cancer Inst 2000, 92:143–147
26. Leenders WP, Kusters B, de Waal RM: Vessel co-option: how tumors obtain blood supply in the absence of sprouting angiogenesis. Endothelium 2002, 9:83–87
27. Gerber SA, Moran JP, Frelinger JG, Frelinger JA, Fenton BM, Lord EM: Mechanism of IL-12 mediated alterations in tumour blood vessel morphology: analysis using whole-tissue mounts. Br J Cancer 2003, 88:1453–1461
28. Gerber SA, Turner MJ, Lugade AA, Moran JP, Frelinger JG, Lord EM: Characterization of a lymph node within the mouse prostate: detailed analysis using whole mount histology. Prostate 2005, 63:105–116
29. Bigelow CE, Conover DL, Foster TH: Confocal fluorescence spectroscopy and anisotropy imaging system. Opt Lett 2003, 28:695–697
30. Lee J, Fenton BM, Koch CJ, Frelinger JG, Lord EM: Interleukin 2 expression by tumor cells alters both the immune response and the tumor microenvironment. Cancer Res 1998, 58:1478–1485
31. Carmeliet P, Jain RK: Angiogenesis in cancer and other diseases. Nature 2000, 407:249–257
32. Yancopoulos GD, Davis S, Gale NW, Rudge JS, Wiegand SJ, Holash J: Vascular-specific growth factors and blood vessel formation. Nature 2000, 407:242–248
33. Fonsatti E, Maio M: Highlights on endoglin (CD105): from basic findings towards clinical applications in human cancer. J Transl Med 2004, 2:18–24
34. Sanchez-Elsner T, Botella LM, Velasco B, Langa C, Bernabeu C: Endoglin expression is regulated by transcriptional cooperation between the hypoxia and transforming growth factor-beta pathways. J Biol Chem 2002, 277:43799–43808
35. Jerdan JA, Michels RG, Glaser BM: Extracellular matrix of newly forming vessels—an immunohistochemical study. Microvasc Res 1991, 42:255–265
36. Baluk P, Morikawa S, Haskell A, Mancuso M, McDonald DM: Abnormalities of basement membrane on blood vessels and endothelial sprouts in tumors. Am J Pathol 2003, 163:1801–1815
37. Egginton S, Zhou AL, Brown MD, Hudlicka O: Unorthodox angiogenesis in skeletal muscle. Cardiovasc Res 2001, 49:634–646
38. Ferrara N, Gerber HP, LeCouter J: The biology of VEGF and its receptors. Nat Med 2003, 9:669–676
39. Gerhardt H, Golding M, Fruttiger M, Ruhrberg C, Lundkvist A, Abramsson A, Jeltsch M, Mitchell C, Alitalo K, Shima D, Betsholtz C: VEGF guides angiogenic sprouting utilizing endothelial tip cell filopodia. J Cell Biol 2003, 161:1163–1177
40. Xiong M, Elson G, Legarda D, Leibovich SJ: Production of vascular endothelial growth factor by murine macrophages: regulation by hypoxia, lactate, and the inducible nitric oxide synthase pathway. Am J Pathol 1998, 153:587–598
41. Ramanathan M, Giladi A, Leibovich SJ: Regulation of vascular endothelial growth factor gene expression in murine macrophages by nitric oxide and hypoxia. Exp Biol Med (Maywood) 2003, 228:697–705
42. Cui L, Johkura K, Liang Y, Teng R, Ogiwara N, Okouchi Y, Asanuma K, Sasaki K: Biodefense function of omental milky spots through cell adhesion molecules and leukocyte proliferation. Cell Tissue Res 2002, 310:321–330
43. Gardner MJ, Jones LM, Catterall JB, Turner GA: Expression of cell adhesion molecules on ovarian tumour cell lines and mesothelial cells, in relation to ovarian cancer metastasis. Cancer Lett 1995, 91:229–234
44. Bot J, Whitaker D, Vivian J, Lake R, Yao V, McCauley R: Culturing mouse peritoneal mesothelial cells. Pathol Res Pract 2003, 199:341–344
45. Burke B, Tang N, Corke KP, Tazzyman D, Ameri K, Wells M, Lewis CE: Expression of HIF-1alpha by human macrophages: implications for the use of macrophages in hypoxia-regulated cancer gene therapy. J Pathol 2002, 196:204–212

46. Lord EM, Harwell L, Koch CJ: Detection of hypoxic cells by monoclonal antibody recognizing 2-nitroimidazole adducts. Cancer Res 1993, 53:5721–5726
47. Koch CJ, Evans SM, Lord EM: Oxygen dependence of cellular uptake of EF5 [2-(2-nitro-1H-imidazol-1-yl)-N-(2,2,3,3,3-pentafluoropropyl)acet amide]: analysis of drug adducts by fluorescent antibodies vs bound radioactivity. Br J Cancer 1995, 72:869–874
48. Lopes Cardozo AM, Gupta A, Koppe MJ, Meijer S, van Leeuwen PA, Beelen RJ, Bleichrodt RP: Metastatic pattern of CC531 colon carcinoma cells in the abdominal cavity: an experimental model of peritoneal carcinomatosis in rats. Eur J Surg Oncol 2001, 27:359–363
49. Williams RHW: The greater omentum: its applicability to cancer surgery and cancer therapy. Curr Probl Surg 1986, 23:789–865
50. Folkman J: Tumor angiogenesis: therapeutic implications. N Engl J Med 1971, 285:1182–1186
51. Holash J, Maisonpierre PC, Compton D, Boland P, Alexander CR, Zagzag D, Yancopoulos GD, Wiegand SJ: Vessel cooption, regression, and growth in tumors mediated by angiopoietins and VEGF. Science 1999, 284:1994–1998
52. Zhang QX, Magovern CJ, Mack CA, Budenbender KT, Ko W, Rosengart TK: Vascular endothelial growth factor is the major angiogenic factor in omentum: mechanism of the omentum-mediated angiogenesis. J Surg Res 1997, 67:147–154
53. Pond CM: Paracrine interactions of mammalian adipose tissue. J Exp Zool Part A Comp Exp Biol 2003, 295:99–110
54. Mutsaers SE: The mesothelial cell. Int J Biochem Cell Biol 2004, 36:9–16
55. Visser CE, Tekstra J, Brouwer-Steenbergen JJ, Tuk CW, Boorsma DM, Sampat-Sardjoepersad SC, Meijer S, Krediet RT, Beelen RH: Chemokines produced by mesothelial cells: huGRO-alpha, IP-10, MCP-1 and RANTES. Clin Exp Immunol 1998, 112:270–275
56. Kinnaert P, De Wilde JP, Bournonville B, Husson C, Salmon I: Direct activation of human peritoneal mesothelial cells by heat-killed microorganisms. Ann Surg 1996, 224:745–754
57. Mohammed KA, Nasreen N, Hardwick J, Logie CS, Patterson CE, Antony VB: Bacterial induction of pleural mesothelial monolayer barrier dysfunction. Am J Physiol 2001, 281:L119–L125
58. Gary Lee YC, Melkerneker D, Thompson PJ, Light RW, Lane KB: Transforming growth factor beta induces vascular endothelial growth factor elaboration from pleural mesothelial cells in vivo and in vitro. Am J Respir Crit Care Med 2002, 165:88–94
59. Lessan K, Aguiar DJ, Oegema T, Siebenson L, Skubitz AP: CD44 and beta1 integrin mediate ovarian carcinoma cell adhesion to peritoneal mesothelial cells. Am J Pathol 1999, 154:1525–1537
60. Takatsuki H, Komatsu S, Sano R, Takada Y, Tsuji T: Adhesion of gastric carcinoma cells to peritoneum mediated by alpha3beta1 integrin (VLA-3). Cancer Res 2004, 64:6065–6070
61. Tietze L, Borntraeger J, Klosterhalfen B, Amo-Takyi B, Handt S, Gunther K, Merkelbach-Bruse S: Expression and function of beta(1) and beta(3) integrins of human mesothelial cells in vitro. Exp Mol Pathol 1999, 66:131–139